In Silico Pharmacological Analysis of a Potent Anti-Hepatoma Compound of Mushroom Origin and Emerging Role as an Adjuvant Drug Lead

13 authors, including:

Achyut Adhikari
Tribhuvan University
130 PUBLICATIONS   910 CITATIONS

Kanishka Senathilake
University of Colombo
11 PUBLICATIONS   69 CITATIONS

E. Dilip de Silva
University of Colombo
186 PUBLICATIONS   2,443 CITATIONS

Chandrika Nanayakkara
University of Colombo
81 PUBLICATIONS   222 CITATIONS

Some of the authors of this publication are also working on these related projects:

Searching for lead compounds from Sri Lankan endemic plants that targets breast cancer stem cells View project

Screening Sri Lankan macrofungi for health related targets View project

![Scientific Research Publishing logo]

In Silico Pharmacological Analysis of a Potent Anti-Hepatoma Compound of Mushroom Origin and Emerging Role as an Adjuvant Drug Lead

Muthuthanthriege Dilusha Maduranganie Fernando[1], Achyut Adhikari[2*],
Nambukara Helambage Kanishka Sithira Senathilake[3], Egodage Dilip de Silva[3],
Chandrika Malkanthi Nanayakkara[4], Ravindra Lakshman Chundananda Wijesundera[4],
Preethi Soysa[5], Babaranda Gammacharige Don Nissanka Kolitha de Silva[1*]

[1]Centre for Biotechnology, Department of Zoology, Faculty of Applied Sciences, University of Sri Jayewardenepura, Nugegoda, Sri Lanka
[2]Central Department of Chemistry, Tribhuvan University, Kritipur, Nepal
[3]Institute of Biochemistry, Molecular Biology and Biotechnology, University of Colombo, Colombo, Sri Lanka
[4]Department of Plant Sciences, Faculty of Science, University of Colombo, Colombo, Sri Lanka
[5]Department of Biochemistry and Molecular Biology, Faculty of Medicine, University of Colombo, Colombo, Sri Lanka
Email: *achyutraj05@gmail.com, *nissanka@sci.sjp.ac.lk

Abstract

Mushrooms are well-known to possess a continuum of anticancer metabolites that are vital in the development of anticancer adjuvant drug leads based on natural products. Owing to the fact that conventional cancer therapeutic methods were failed to lessen mortality caused by cancer to the estimated level with occurrence of adverse side effects, anticancer agents isolated from natural mushroom sources unarguably make an experimental research area worth mass focus today. The current study was targeted on *in vitro* cytotoxicity and *in silico* predictive pharmacological analysis of a flavonoid compound isolated from *Fulvifomes fastuosus* mushroom. Targeted compound was isolated from the mushroom using different chromatographic methods and identified by NMR spectrometry and mass spectrometry. Cytotoxicity experiments were carried out using MTT assay and apoptotic cells were identified by ethidium bromide/acridine orange staining. The SwissADME tool, BOILED-Egg construction model and Swiss target protein prediction software have been used to perform *in silico* predictive pharmacological analysis. The isolated compound has been identified as 2-(3,4-dihydroxyphenyl)-6-[(E)-2-(3,4-dihydroxyphenyl)ethenyl]-5'-methylspiro[2H-furo[3,2-c]pyran-3,2'-furan]-3',4-dione by spectrometric methods. The result of MTT assay showed that 2-(3,4-dihydroxyphenyl)-6-[(E)-2-(3,4-dihydroxyphenyl)ethenyl]-5'-methylspiro[2H-furo[3,2-c]pyran-3,2'-furan]-3',4-dione has potent anticancer activity for hepatoma

against Hep-G2 cell line (IC$_{50}$ = 20.8 μg/ml) being less toxic to normal CC-1 epithelial cells (IC$_{50}$ = 167.00 μM). The cells treated with compound exhibited apoptotic features such as cellular shrinkage, nuclear fragmentation and condensed cytoplasm. In summary, 2-(3,4-dihydroxyphenyl)-6-[(E)-2-(3,4-dihydroxyphenyl)ethenyl]-5'-methylspiro[2H-furo[3,2-c]pyran-3,2'-furan]-3',-4-dione has shown potent anticancer properties against hepatoma with less cytotoxicity effect on normal cells. Furthermore, *in silico* study has revealed that properties of 2-(3,4-dihydroxyphenyl)-6-[(E)-2-(3,4-dihydroxyphenyl)ethenyl]-5'-methylspiro[2H-furo[3,2-c]pyran-3,2'-furan]-3',4-dione may contribute to making a high absorption and clearance of the test compound as not interfering with the therapeutic failure of the compound. The properties of 2-(3,4-dihydroxyphenyl)-6-[(E)-2-(3,4-dihydroxyphenyl)ethenyl]-5'-methylspiro [2H-furo-[3,2-c]pyran-3,2'-furan]-3',4-dione were compatible with well-known anticancer drug lapatinib. In conclusion, 2-(3,4-dihydroxyphenyl)-6-[(E)-2-(3,4-dihydroxyphenyl)ethenyl]-5'-methylspiro[2H-furo[3,2-c]pyran-3,2'-furan]-3',4-dione has a high tendency to act as a good anticancer adjuvant drug in the treatment of hepatoma.

1. Introduction

It is well reputable that the use of medicinal mushrooms provides advantageous effects on human well-being mainly due to its therapeutic value [1]. The utilization of mushroom products as a source of medication has been commenced more than 100 years ago as they are enormously rich in biologically active secondary metabolites. Among 14,000 of mushroom species that have been identified yet, about 650 species of mushrooms have been reported to possess promising anticancer activity [2] [3]. Bioactive compounds isolated from mushrooms with anticancer properties have been identified to contain polysaccharides, polysaccharide-protein complexes, dietary fiber, certain types of proteins, phenols, terpenoids, flavonoids and steroids etc. [3] [4]. Nowadays, a major challenge encountered by the entire world community is to uncover a feasible strategy to fight neoplastic diseases as cancer is still a chronic disease that causes severe death or long term effects throughout the life [4]. Plentiful side effects given by conventional therapies to treat cancer including surgery, chemotherapy, and radiation therapy, promote the use of additional therapy to retain and improve the immune status of patients [5]. Scientists made it feasible with introduction of the use of natural drugs with conventional therapy as an adjuvant treatment, especially those that have cytotoxic activity with minor side effects. For instance, lentinan, schizophyllan and krestin are natural compounds which were isolated from *Lentinus edodes*, *Schizophyllum commune* and *Trametes versicolor* mu-

shrooms species. All these metabolites have passed clinical trials and approved as prescribed cancer drugs in Japan to use them in adjuvant cancer therapy [6].

It is worth to note, that clinical trials for mushroom originated drugs are sufficiently expensive and long-term. Hence, researchers have done plenty of investigations for anticancer activity of medicinal mushrooms *in vitro* and *in vivo*. However, most of the drugs have been passed clinical trials. Initial phases of clinical trials for these drugs exhibit great anticancer activity with absence of immediate or long-term toxicity [7] [8].

In spite of the potency of the natural anticancer compounds isolated from mushrooms, they must reach the target in the human body in adequate concentration, and reside there in a bioactive form long enough for the execution of expected biologic events to be effective as a drug. Hence, drug development process of a potent molecule involves assessment of absorption, distribution, metabolism and excretion (ADME) of that targeted substance inside the body [9]. *In silico* methods have been fostered as valid substitutes to experimental procedures for prediction of ADME, particularly at initial steps, when investigated substances are abundant but the availability of compounds is scarce [9].

In silico toxicology is one form of toxicity assessment which uses computational resources such as methods, algorithms, software, data, etc., in order to analyze, organize, simulate, model and predict toxicity of chemical substances [10]. It is knotted with *in silico* pharmacology, which uses data through computational tools to analyze beneficial or harmful effects of drugs in therapeutic purposes [11]. Computational methods are targeted to complement *in vitro* and *in vivo* toxicity experiments to potentially minimize the necessity for animal testing. Moreover, it aims to lessen the cost and time required for animal experiments and safety assessment [12]. Drug discovery is a multifarious process with the aim of determining efficacious molecules where their selectivity and strength are balanced with absorption, distribution, metabolism, excretion and toxicity (ADMET) properties to find out the fitting dose and dosing interval [13]. The connection between physicochemical properties and molecular structure is well known. The link between physicochemical properties and a drug's biological behavior exhibits an indirect relationship back to structure. It facilitates the prediction of a biological property using particular molecular manipulation [14]. In the point of minimizing wasted drug discovery efforts and prevention of the synthesis of high risk compounds, computational methods are used to predict the physicochemical properties accurately.

In this study, ADMET behaviors of key physicochemical properties, such as ionization, hydrophobicity, solubility, hydrogen bonding strength will be predicted *in silico* using SwissADME web tool [15]. Detailed analyses of the binding characteristics lead to ranking of the targets according to the tightness of binding [16]. This study will be also targeted a *in silico* study of drug likeliness of the isolated compound which is useful in the identification of drug targets related to hepatoma and prediction of binding-conformation of small molecule ligands to

the target binding site [16]. Swiss target prediction software is used to predict target proteins for the isolated test molecule. The BOILED-Egg construction model is used via SWISSADME to assess the gastrointestinal absorption and brain penetration of the targeted compound. Gastrointestinal absorption and brain penetration data are standardized by this model and subjected to lipophilicity (WLOGP) and polarity (tPSA) computation [16].

2. Materials and Methods

2.1. Fungal Material

The specimen of *F. fastuosus* was collected from the dry zone forest reserves of Sigiriya and Dambulla in Sri Lanka during the period of September 2012 to October 2013. Specimens were transported to the laboratory with proper ventilation. The identity of the specimen was achieved by a botanist of Department of Plant Science, Faculty of Science, University of Colombo and molecular studies has confirmed the identity of the species (Genbank Accession No.: KP757737). Voucher specimens were deposited at the same Institute (UOC:DAMIA:D27b).

2.2. Large Scale Extraction of Fruiting Bodies of *F. fastuosus*

Mature fruiting bodies of *F. fastuosus* were cleaned, dried in the oven at 40°C to a constant mass and pulverized. Shredded and ground mushroom specimen of fruiting bodies from *F. fastuosus* (1 kg) was subjected to sonication extraction with methanol (4 L), for 5 - 6 hours at 37°C. Methanol extract was filtered twice through Whatman No. 1 filter paper and same extraction procedure was repeated for three times. Filtrates were pooled and evaporated to dryness at 40°C under reduced pressure using rotary evaporator. The resulting dried methanol extract was dissolved in distilled water (500 mL) with maximum solubility and partitioned into hexane by liquid-liquid extraction. Remainder in water was partitioned into dichloromethane. Dichloromethane layer was dispensed and aqueous layer was extracted into ethyl acetate using same extraction procedure. Ethyl acetate fraction was evaporated in a rotary evaporator to yield dried extract.

2.3. Isolation of Test Compound by Normal Phase Column Chromatography

The ethyl acetate extract was fractionated by normal phase column chromatography using the following protocol. The dried ethyl acetate extract was dissolved in a minimum amount of methanol and added to 50 g of silica gel (230 - 400 mesh, 60 Å). The resulting silica gel slurry was then dried using rotary evaporation and placed at the top of 50 mm diameter column producing a final bed height of 200 mm. The column of silica was eluted, using a gradient solvent system starting from 1:1 ethyl acetate: hexane to 4:1 ethyl acetate: hexane (300 ml each in 5% step gradient), yielded fractions (25 ml each) number 20 - 23 was comprised the targeted compound and evaporated the preferred fractions by air-drying. Dried fractions were further washed with acetone to remove any

contaminations and spotted on silica gel plates to give a consolidated under 365 nm UV lamp. Further purifications were performed using reverse phase preparative HPLC to obtain the purified product of the targeted compound.

2.4. Purification by High Performance Liquid Chromatography (HPLC)

Dried compound was further purified by a recycling preparative-HPLC (Model LC-908, JAI Co., Japan) eluting with a linear gradient from 9:1 to 3:7 water:methanol acidified with 0.04% trifluoroacetic acid at a flow rate of 5 mL/min. Prime sphere C_{18} HC (10 g) 50×250 mm with a 50×30 mm guard column was used in the preparative HPLC. In this manner, purified HPLC fraction comprising the compound 2-(3,4-dihydroxyphenyl)-6-[(E)-2-(3,4-dihydroxyphenyl)ethenyl]-5'-methylspiro[2H-furo[3,2-c]pyran-3,2'-furan]-3',4-dione was obtained in substantially purified form (≥98%) and the product can be dried using freeze-drying methods to obtain the amorphous yellow colour powder of 2-(3,4-dihydroxyphenyl)-6-[(E)-2-(3,4-dihydroxyphenyl)ethenyl]-5'-methylspiro[2H-furo[3,2-c]pyran-3,2'-furan]-3',4-dione. All chromatographic runs were performed at ambient temperature using HPLC grade solvents.

2.5. Identification and Characterization of the Compound by Nuclear Magnetic Resonance (NMR)

Nuclear magnetic resonance (NMR) spectra were recorded on a Bruker avance AV—400 or 500 MHz spectrometer in deuterated acetone: methanol (1:1) mixture. One and two-dimensional NMR experiments, including ^{1}H-NMR (proton NMR), ^{13}C-NMR, DEPT[13]C-NMR (Distortionless Enhancement Polarization Transfer ^{13}C-NMR), H-H Correlation Spectroscopy (COSY), Heteronuclear Single Quantum Correlation (HSQC), Heteronuclear Multiple Bond Correlation (HMBC), Nuclear Overhauser Effect Spectroscopy (NOESY) provided molecular structure information. In addition, HREIMS (High Resolution Electrospray Ionization Mass Spectrometry) was performed to obtain the high resolution mass spectrum.

2.6. Cell Lines and Cell Culture

Hep-G2 and CC-1 cell lines (ATCC) were cultured in DMEM supplemented with 10% heat inactivated fetal bovine serum (FBS), 3% glutamine, sodium bicarbonate and antibiotic (penicillin/ streptomycin). The cells were incubated at 37˚C in a humidified CO_2 incubator.

Determination of Cytotoxicity Effect of 2-(3,4-dihydroxyphenyl)-6-[(E)-2-(3,4-dihydroxyphenyl)ethenyl]-5'-methylspiro[2H-furo[3,2-c]pyran-3,2'-furan]-3',4-dione for Hepatoma and CC-1 Cell Lines Using MTT Assay

Antiproliferative activities of 2-(3,4-dihydroxyphenyl)-6-[(E)-2-(3,4-dihydroxyphenyl)ethenyl]-5'-methylspiro[2H-furo[3,2-c]pyran-3,2'-furan]-3',4-dione against hepatoma and CC-1 cells were determined using MTT (3,4,5-(dimethyl-thiazol-2-yl)2-5-diphenyl tetrazolium bromide) assay. Metabolically active cells reduce

MTT in to purple colored formazan crystals. Adherent cell lines were transferred with 0.12% trypsin and 0.5% EDTA and cells (2×10^5 cells/well) were seeded in 24-well plates and incubated overnight with 1 mL of the DMEM medium described above. The stock solution of the test compound was prepared in DMSO at a concentration of 1 mg/ml and subsequently diluted up to 1000 ng/ml in order to prepare the working standards. The resulting monolayers of Hep-G2 cells and CC-1cells (70% confluence) were treated with different concentrations of the test solution and incubated for 24 hours at 37°C.

In all experiments, cycloheximide (5 mM, 50 μl) was used as the positive control and negative control contained 0.25% DMSO in growth media. The culture medium was replaced with fresh medium (1 ml) after 24 hours and MTT (5 mg/ml; 100 μl) was added to each well. The cells were incubated at 37°C for 3 hours and the medium was aspirated carefully. The remaining formazan crystals were solubilized with 750 μl of 0.05 M HCl (in 2-propanol) and absorbance was measured at 570 nm. The absorbance given by the solution was measured at 570 nm.

1) Determination of IC$_{50}$ value

Percentage cell viability was calculated using the formula: Percentage cell viability = [(Absorbance of untreated cells − Absorbance of treated cells)/Absorbance of untreated cells] × 100. The net absorbance from the wells of the untreated cells (negative control) was taken as the 100% viability. IC$_{50}$ of the test solution against Hep-G2 cells was determined by regression analysis of the corresponding dose response curve.

2) Determination of selectivity index

CC$_{50}$ of the test solution against CC-1 cells was determined using the regression analysis of the corresponding dose response curve. Safety of the compound against normal cells was determined in terms of selectivity index (SI) by calculating the ratio of CC$_{50}$/IC$_{50}$ (SI value > 2 is considered as safe) [17].

2.7. Morphological Determination and DNA Fragmentation of Apoptosed Cells

The morphological changes of treated Hep-G2 and CC-1 cells with different concentrations of the test solution over 24 hours were detected by microscopic examination of cells. Morphological changes of the cells treated with negative and positive controls were compared under phase contrast microscope.

Acridine Orange/Ethidium Bromide Staining of Apoptosed Cells

Hep-G2 (2×10^3 cells/well) and CC-1 cells (2×10^2 cells/well) were seeded in chamber slides and resulting confluent layers were treated with different concentrations of the test solution and incubated at 37°C for 24 hours. The adherent cells were washed with 200 μL of PBS and 2 μL of the dye mixture of ethidium bromide (100 mg/mL) and acridine orange (100 mg/mL) in 1:1 ratio was placed on each well of the chamber slide. Chamber slides were observed immediately under the fluorescence microscope. Images were photographed using a Nikon D

700 camera connected to the microscope.

2.8. Determination of *in Silico* Pharmacokinetic, Physicochemical Parameters and Drug Likeliness of the Compound

2.8.1. SwissADME Web Tool

Assessment of *in silico* pharmacokinetic parameters, physicochemical parameters, drug likeliness, lipophilicity and medicinal chemistry friendliness properties for the molecule were performed using SwissADME web tool.

2.8.2. BOILED-Egg Construction Model

The BOILED-Egg construction model was obtained via SWISSADME to assess the gastrointestinal absorption and brain penetration of the targeted compound. This model standardizes gastrointestinal absorption and brain penetration data-sets and converts into SMILES notation which in turn subjected to lipophilicity (WLOGP) and polarity (tPSA) computation.

2.8.3. Prediction of Target Proteins of the Compound

The target proteins for the isolated molecule have been predicted using the Swiss target prediction software. Interactions were selected based on following criteria; I) involve human proteins (II) annotate as direct binding with an activity (K_i, K_d, IC_{50} or EC_{50}) ≤ 10 μM (III) involve molecules consisting of 80 heavy atoms and (IV) involve targets that are single proteins or protein complexes.

2.9. Calculations and Statistics

All experiments were carried out in triplicate and set values are representative for at least three independent experiments. All the results of the experiments were presented as the mean ± standard deviation (Mean ± SD). The results were statistically analyzed by SPSS statistic software package. A p-value less than 0.05 was considered as statistically significant.

3. Result and Discussion

3.1. Structure Elucidation of the Flavonoid Compound Isolated from *Fulviformes fastuosus*

The spectroscopic methods including 1D and 2D NMR experiments were used to identify the chemical structure of the isolated compound. It was confirmed as 2-(3,4-dihydroxyphenyl)-6-[(E)-2-(3,4-dihydroxyphenyl)ethenyl]-5'-methylspiro-[2H-furo[3,2-c]pyran-3,2'-furan]-3',4-dione (**Figure 1**) with $C_{25}H_{18}O_9$, molecular formula and m/z 462 g/mol as determined by HREIMS (High resolution electrospray ionization mass spectrometry) and by combination of the ^{1}H-NMR (proton NMR), ^{13}C-NMR, DEPT[13]C-NMR (Distortionless Enhancement Polarization Transfer ^{13}C NMR), Heteronuclear Multiple Bond Correlation (HMBC), Heteronuclear Multiple Quantum Correlation (HMQC), H-H Correlat17ion Spectroscopy (COSY) and Nuclear Overhauser effect spectroscopy (NOESY). **Table 1** shows the assigned ^{13}C and ^{1}H chemical shifts for the isolated compound.
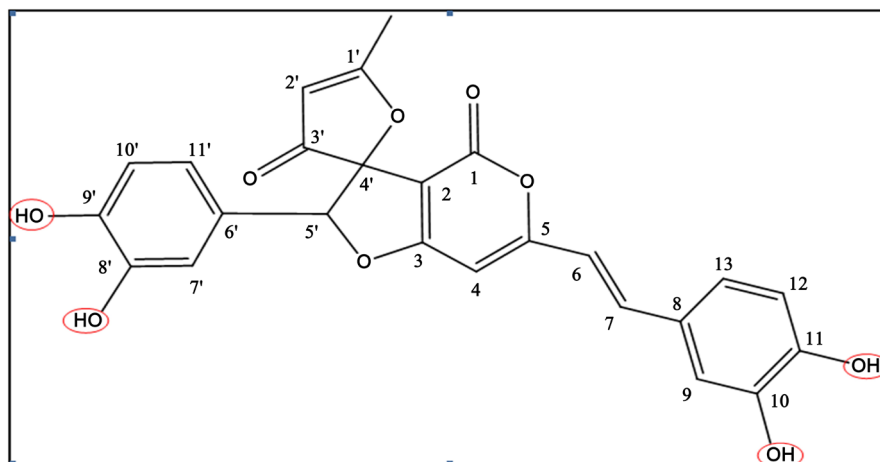
Figure 1. The structural formula of 2-(3,4-dihydroxyphenyl)-6-[(E)-2-(3,4-dihydroxyphenyl)ethenyl]-5'-methylspiro[2H-furo[3,2-c]pyran-3,2'-furan]-3',4-dione. The red colour circles indicate four hydroxy groups that can be derivatized to produce analogs of 2-(3,4-dihydroxyphenyl)-6-[(E)-2-(3,4-dihydroxyphenyl)ethenyl]-5'-methylspiro[2H-furo[3,2-c]pyran-3,2'-furan]-3',4-dione.

Table 1. ^{13}C-and ^{1}H-NMR chemical shift values of 2-(3,4-dihydroxyphenyl)-6-[(E)-2-(3,4-dihydroxyphenyl)ethenyl]-5'-methylspiro[2H-furo[3,2-c]pyran-3,2'-furan]-3',4-dione (ppm, CD$_3$OD + (CD$_3$)$_2$CO, 600 and 400 MHz respectively).

C. No.	δ_C	δ_H (J, Hz)
1	160.3	-
2	99.7	-
3	176.6	6.51
4	95.8	-
5	166.9	6.75 d (15.6)
6	116.8	7.43 d (15.6)
7	139.7	-
8	128.5	-
9	115.1	7.08 br s
10	149.4	-
11	147.8	-
12	116.6	6.79 d (8.4)
13	122.6	7.01 br d (8.4)
1'	192.6	-
2'	105.1	5.57 s
3'	202.8	-
4'	95.5	-
5'	95.6	5.65 s
6'	123.2	-
7'	115.9	6.76 br s
8'	146.9	-
9'	146.3	-
10'	115.5	6.72 d (8.4)
11'	120.3	6.59 br d (8.4)

The spectral data obtained for the isolated compound were in good agreement with previously reported data for the flavonoid compound 2-(3,4-dihydroxyphenyl)-6-[(E)-2-(3,4-dihydroxyphenyl)ethenyl]-5'-methylspiro[2H-furo[3,2-c]pyran-3,2'-furan]-3',4-dione from the methanolic extract of *Inonotus xeranticus* by Kim J, Yun B, Shim YK, Yoo I (1999) [18].

The structure of the isolated compound 2-(3,4-dihydroxyphenyl)-6-[(E)-2-(3,4-dihydroxyphenyl)ethenyl]-5'-methylspiro[2H-furo[3,2-c]pyran-3,2'-furan]-3',4-dione's structure is indicated in Figure 1.

2-(3,4-dihydroxyphenyl)-6-[(E)-2-(3,4-dihydroxyphenyl)ethenyl]-5'-methylspiro[2H-furo[3,2-c]pyran-3,2'-furan]-3',4-dione possesses interesting structural properties. It is highly oxygenated and functionalized aromatic compound that possess a basic structural unit, namely, the 6-[2-(3,4-dihydroxyphenyl) ethenyl]-4-hydroxy-2H-pyran-2-one (hispidin) moiety. The four hydroxy groups that are circled in red can be derivatized as polyethylene glycol (PEG) esters to give analogs of the targeted compound. Biochemical studies have demonstrated, PEGs are practically nontoxic after acute oral exposure with animals LD_{50} values generally greater than 2000 mg/kg [19]. Apart from this, this compound can be biosynthesized via rearrangement of interfungins A, which is resulted from the condensation of hispidin and hispolon moieties (Figure 2).

3.2. Determination of *in Vitro* Cytotoxicity of Isolated Compound 2-(3,4-dihydroxyphenyl)-6-[(E)-2-(3,4-dihydroxyphenyl)ethenyl]-5'-methylspiro[2H-furo[3,2-c]pyran-3,2'-furan]-3',4-dione

3.2.1. Cytotoxicity of 2-(3,4-dihydroxyphenyl)-6-[(E)-2-(3,4-dihydroxyphenyl)ethenyl]-5'-methylspiro[2H-furo[3,2-c]pyran-3,2'-furan]-3',4-dione against Hep-G2 Cell Line

2-(3,4-dihydroxyphenyl)-6-[(E)-2-(3,4-dihydroxyphenyl)ethenyl]-5'-methylspiro[2H-furo[3,2-c]pyran-3,2'-furan]-3',4-dione have exhibited a strong cytotoxicity against Hep-G2 cell line with lower IC_{50} value in a dose-dependent manner. Cycloheximide (positive control) showed 76% growth inhibition at the concentration of 5 mM (50 μL), while, 2-(3,4-dihydroxyphenyl)-6-[(E)-2-(3,4-dihydroxyphenyl)ethenyl]-5'-methylspiro[2H-furo[3,2-c]pyran-3,2'-furan]-3',4-dione demonstrated a linear relationship of dose dependent increase of cytotoxicity (Figure 3). Moreover, this notable activity was further confirmed by the IC_{50} of 20.8 ± 2.22 μg/ml determined for the mean of the three independent test sample solution against Hep-G2 cell line.

3.2.2. Cytotoxicity of 2-(3,4-dihydroxyphenyl)-6-[(E)-2-(3,4-dihydroxyphenyl)ethenyl]-5'-methylspiro[2H-furo[3,2-c]pyran-3,2'-furan]-3',4-dione against CC-1 Cell Line

The test solution of 2-(3,4-dihydroxyphenyl)-6-[(E)-2-(3,4-dihydroxyphenyl)ethenyl]-5'-methylspiro[2H-furo[3,2-c]pyran-3,2'-furan]-3',4-dione showed less cytotoxicity against CC-1 cell line. Figure 4 depicts that IC_{50} value obtained for the mean of three independent sample preparations of test solution dissolved in DMSO against normal CC-1 cells was 167.00 ± 2.55 μM. In this manner, high

selectivity index of 3.86 has shown by the test compound against Hep-G2 cells and normal cells. Further, this conveys that 2-(3,4-dihydroxyphenyl)-6-[(E)-2-(3,4-dihydroxyphenyl)ethenyl]-5'-methylspiro[2H-furo[3,2-c]pyran-3,2'-furan]-3',4-dione isolated from *Fulvifomes fastuosus* possess potent anticancer activity (IC_{50} = 20.8 μg/ml) for hepatoma with less cytotoxicity effect on normal CC-1 cells.

3.3. Morphological Changes of Apoptosed Cells

Apoptosis is an orderly process of the terminal morphological and biochemical events of programmed cell death which is represented by the specific changes in
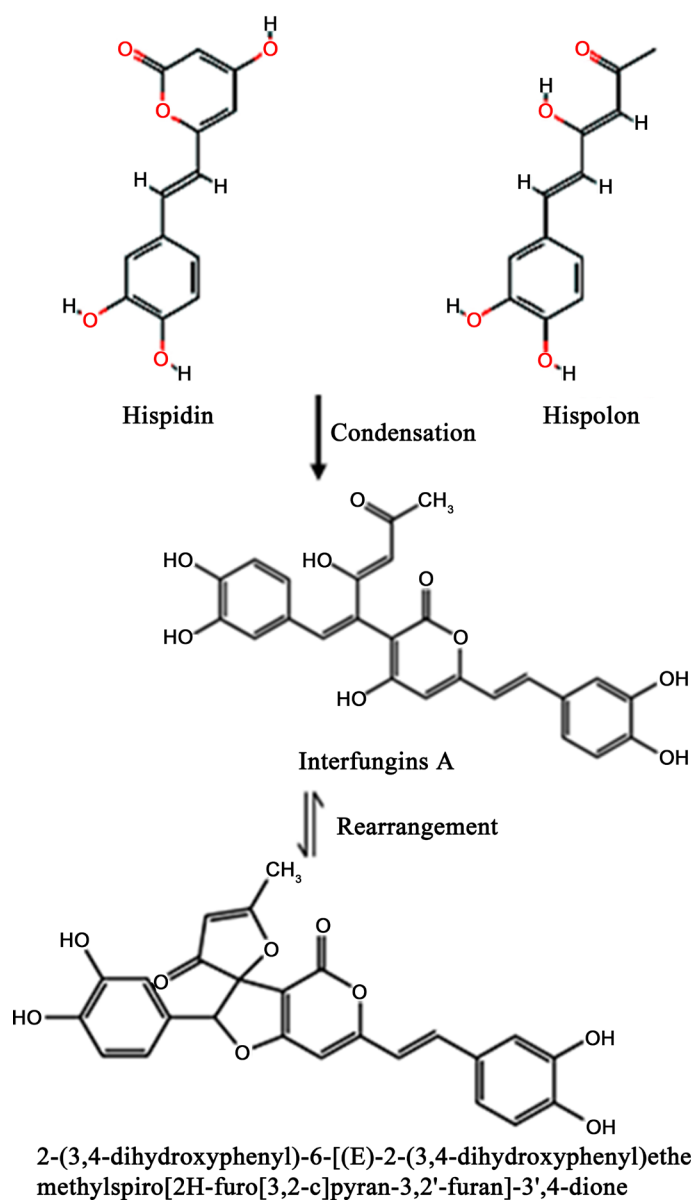

Figure 2. Biosynthetic pathway of 2-(3,4-dihydroxyphenyl)-6-[(E)-2-(3,4-dihydroxyphenyl)-ethenyl]-5'-methylspiro[2H-furo[3,2-c]pyran-3,2'-furan]-3',4-dione via rearrangement of interfungins A, which is resulted from the condensation of hispidin and hispolon moieties.
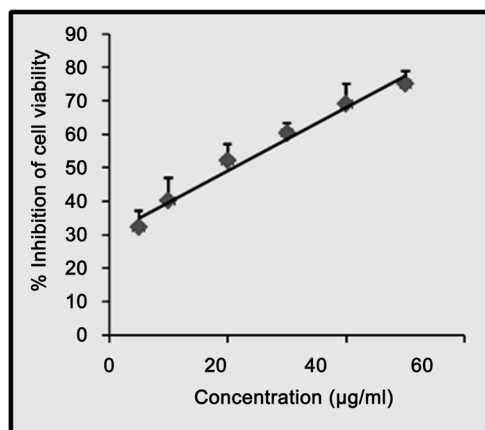
Figure 3. The percentage induction of cytotoxic activity of 2-(3,4-dihydroxyphenyl)-6-[(E)-2-(3,4-dihydroxyphenyl)ethenyl]-5'-methylspiro[2H-furo[3,2-c]pyran-3,2'-furan]-3', 4-dione for Hep-G2 cell line as revealed by MTT assay (24 hour incubation period). The graphical data are represented as mean ± SD of three independent MTT experiments (n = 3).
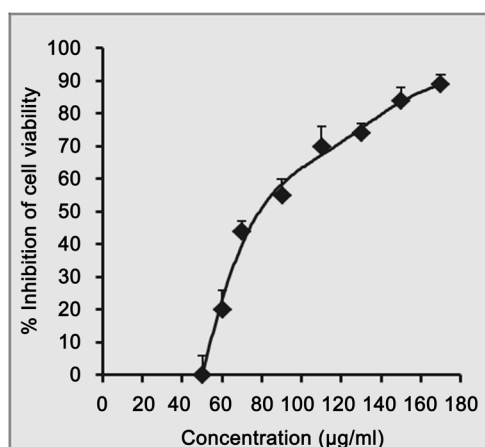

Figure 4. The percentage induction of cytotoxic activity of 2-(3,4-dihydroxyphenyl)-6-[(E)-2-(3,4-dihydroxyphenyl)ethenyl]-5'-methylspiro[2H-furo[3,2-c]pyran-3,2'-furan]-3',4-dione against CC-1 cell line as determined by MTT assay (24 hour incubation period). The graphical data are depicted as mean ± SD of three independent MTT experiments (n = 3).

cell surface and nuclear morphology [20]. The morphological changes that can be observed after undergoing the process of apoptosis are cellular shrinkage, irregular shapes, nuclear fragmentation and condensed cytoplasm. The changes of morphological characteristics of apoptosed Hep-G2 and CC-1 cells after the treatment with targeted compound are indicated in Figure 5 and Figure 6.

Hep-G2 and CC-1 cells treated with higher doses predominantly exhibited apoptotic features including cellular shrinkage, oval or irregular in shape, fragmented nuclei and condensed cytoplasm. Hep-G2 and CC-1 cells treated with the lower concentrations of test solution of compound 2-(3,4-dihydroxyphenyl)-6-[(E)-2-(3,4-dihydroxyphenyl)ethenyl]-5'-methylspiro[2H-furo[3,2-c]pyran-3,2'-furan]-3',4-dione manifested elongated shape.
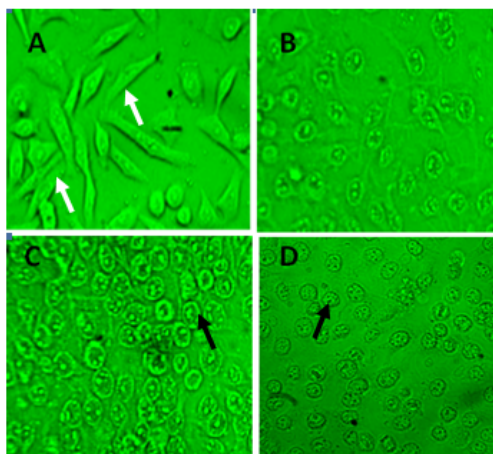
Figure 5. The morphological changes of Hep-G2 cell line treated with 2-(3,4-dihydroxy-phenyl)-6-[(E)-2-(3,4-dihydroxyphenyl)ethenyl]-5'-methylspiro[2H-furo[3,2-c]pyran-3,2'-furan]-3',4-dione test solution for 24 hour incubation at differrent concentrations detected by light microscopy. (A) 0.1 µg/mL; (B) 20 µg/mL; (C) 100 µg/mL; (D) Cyclohex-imide (positive control) 5 mM; 50 µL. White colour arrows show elongated form of the normal cells. Black arrows denote nuclear fragmentation (×400).
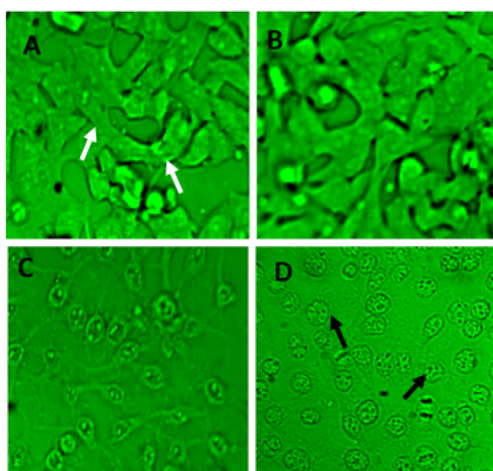

Figure 6. The morphological changes of CC-1 cell line treated with 2-(3,4-dihydroxy-phenyl)-6-[(E)-2-(3,4-dihydroxyphenyl)ethenyl]-5'-methylspiro[2H-furo[3,2-c]pyran-3,2'-furan]-3',4-dione test solution after 24 hour incubation at different concentrations detected by light microscopy. (A) 0.1 µg/mL; (B) 20 µg/mL; (C) 80 µg/mL; (D) Cyclohex-imide (positive control) 5 mM; 50 µL. White colour arrows represent elongated appearance of the normal CC-1 cells. Black arrows show fragmented nuclei (×400).

3.4. Acridine Orange/Ethidium Bromide Staining of Apoptosed Cancerous Cells

Acridine orange-ethidium bromide (AO/EB) fluorescent staining of apoptosed Hep-G2 and CC-1 cells treated with the test solution of 2-(3,4-dihydroxy-phenyl)-6-[(E)-2-(3,4-dihydroxyphenyl)ethenyl]-5'-methylspiro[2H-furo[3,2-c]pyran-3,2'-furan]-3',4-dione were depicted in Figure 7 and Figure 8. Distinctly, the number of apoptotic cells was gradually increased with the treatment dose of the test solution.
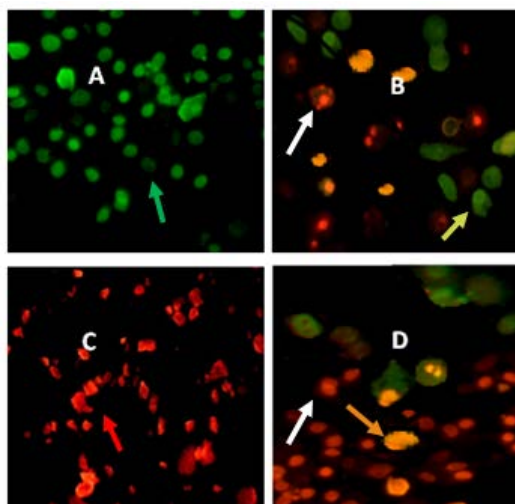
Figure 7. Acridine orange-ethidium bromide (AO/EB) fluorescent staining of Hep-G2 cells treated with 2-(3,4-dihydroxyphenyl)-6-[(E)-2-(3,4-dihydroxyphenyl)ethenyl]-5'-methylspiro[2H-furo[3,2-c]pyran-3,2'-furan]-3',4-dione test solution depicts the apoptotic morphology of Hep-G2 cells. (A) Negative control; (B) 20 μg/μL; (C) 50 μg/mL; (D) Cycloheximide (positive control) 5 mM; 50 μL. Green arrows indicate live cells, greenish yellow shows early apoptotic cells, orange red represents late apoptotic cells, dead cells are represented by red colour. Some cells have fragmented and faded appearance. White colour arrows point out blebbing formation (Original magnification 400×).
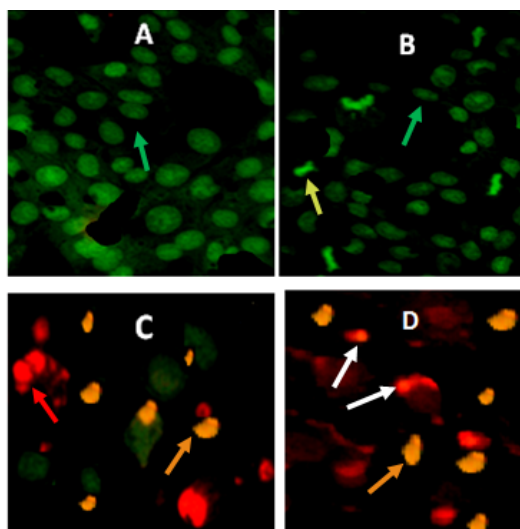
Figure 8. Acridine orange-ethidium bromide (AO/EB) fluorescent staining of CC-1 cells treated with 2-(3,4-dihydroxyphenyl)-6-[(E)-2-(3,4-dihydroxyphenyl)ethenyl]-5'-methylspiro-[2H-furo[3,2-c]pyran-3,2'-furan]-3',4-dione test solution depicts the apoptotic morphology of CC-1 cells. (A) Negative control; (B) 40 μg/mL; (C) 80 μg/mL; (D) Cycloheximide (positive control) 5 mM; 50 μL. Green arrows indicate live cells, greenish yellow shows early apoptotic cells and orange red represents the late apoptotic cells. Dead cells were depicted by red colour. Some cells have fragmented and faded appearance. White arrows indicate blebbing formation (Original magnification 400×).

Figure 7 and Figure 8 illustrate that live cells are represented by nuclei stained with greenish colour while early apoptotic cells are represented by greenish yellow.

Condensed orange red colour nuclei specify late apoptotic cells whereas red colour shows dead cells. The untreated cells of the negative control and treated cells with the lower concentrations of the test solution are appeared with the normal nuclei coloured in bright green. Cells treated with higher doses of the test solution and cells treated with positive control demonstrate distinctive features of apoptosis such as nuclear fragmentation, chromatin condensation, presence of apoptotic bodies and blebbing formation by staining with ethidium bromide/acridine orange. Chromatin condensation and nuclear fragmentation were predominantly observed apoptotic features with high concentrations of the test solution and total number of apoptotic cells was gradually amplified with the treatment dose of the test solution.

3.5. Determination of the *in Silico* Toxicological Parameters of the Isolated Compound Using SwissADME

The SwissADME tool has estimated the key physicochemical, pharmacokinetic, drug-like and and medicinal chemistry friendliness properties for the molecule. This SwissADME section gives access to five different rule-based filters, with diverse ranges of properties inside of which the molecule is defined as drug-like. These filters often originate from analyses by major pharmaceutical companies aiming to improve the quality of their proprietary chemical collections. The Lipinski (Pfizer) filter is the pioneer rule-of-five implemented rules. The Ghose (Amgen), Veber (GSK), Egan (Pharmacia) and Muegge (Bayer) methods have made other 4 rules for drug likeliness. Multiple estimations allow consensus views or selection of methods best fitting the end-user's specific needs in terms of chemical space or project-related demands. Any violation of any rule described here appears explicitly in the output panel [21].

The 2-(3,4-dihydroxyphenyl)-6-[(E)-2-(3,4-dihydroxyphenyl)ethenyl]-5'-methylspiro[2H-furo[3,2-c]pyran-3,2'-furan]-3',4-dione was first described by its chemical structure and canonical SMILES together with the Bioavailability Radar. Bioavailability Radar displays rapid appraisal of drug-likeness [21]. Six physicochemical properties were taken into account: lipophilicity, size, polarity, solubility, flexibility and saturation, pharmacokinetics, drug-likeness and medicinal Chemistry (Figure 9).

SWISS-ADME has analyzed pharmacokinetics parameters including the response towards CYP and P-gp/MDR1proteins that are localized at the apical/luminal membrane of enterocytes [21]. P-gp/MDR1 and CYP3A proteins act as a major protective barrier for the bioavailability of orally administered drugs synergistically. Moreover, P-gp/MDR1 also plays a role in counteracting active transport of drug molecules back to the lumen after it is passively absorbed into the enterocytes [21]. The localization of P-gp/MDR1 and CYP3A represents that the quantity of substrates metabolized by the CYP3A enzyme can be controlled by P-gp/MDR1. The decreased P-gp activity in the intestine causes dramatic increase in the bioavailability of drug substance. Conversely, P-gp activity can be increased due to various factors such as drug interactions or genetic mutations
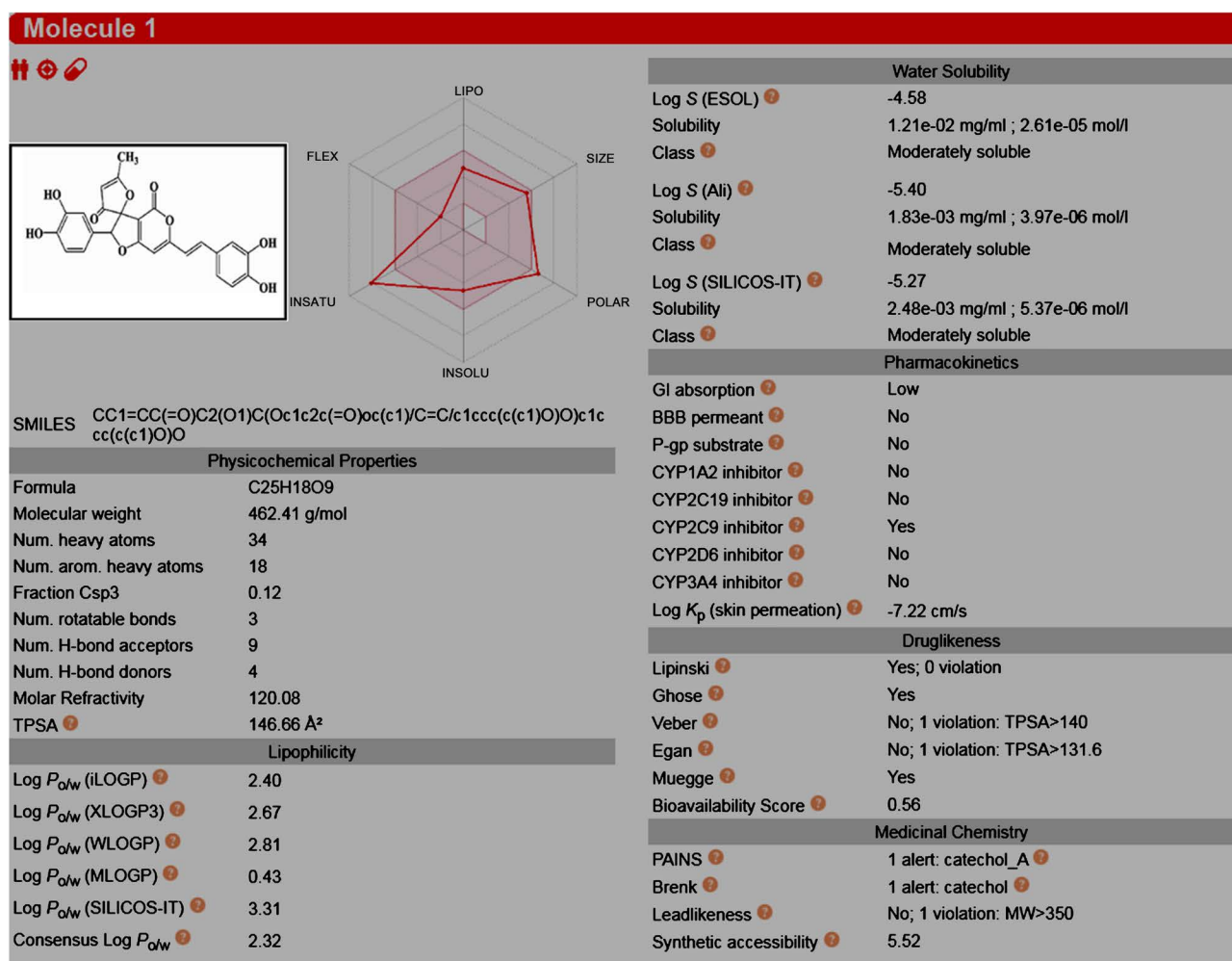
Molecule 1

SMILES CC1=CC(=O)C2(O1)C(Oc1c2c(=O)oc(c1)/C=C/c1ccc(c(c1)O)O)c1cc(c(c1)O)O

Physicochemical Properties

Formula	C25H18O9
Molecular weight	462.41 g/mol
Num. heavy atoms	34
Num. arom. heavy atoms	18
Fraction Csp3	0.12
Num. rotatable bonds	3
Num. H-bond acceptors	9
Num. H-bond donors	4
Molar Refractivity	120.08
TPSA	146.66 Å²

Lipophilicity

Log $P_{o/w}$ (iLOGP)	2.40
Log $P_{o/w}$ (XLOGP3)	2.67
Log $P_{o/w}$ (WLOGP)	2.81
Log $P_{o/w}$ (MLOGP)	0.43
Log $P_{o/w}$ (SILICOS-IT)	3.31
Consensus Log $P_{o/w}$	2.32

Water Solubility

Log S (ESOL)	-4.58
Solubility	1.21e-02 mg/ml ; 2.61e-05 mol/l
Class	Moderately soluble
Log S (Ali)	-5.40
Solubility	1.83e-03 mg/ml ; 3.97e-06 mol/l
Class	Moderately soluble
Log S (SILICOS-IT)	-5.27
Solubility	2.48e-03 mg/ml ; 5.37e-06 mol/l
Class	Moderately soluble

Pharmacokinetics

GI absorption	Low
BBB permeant	No
P-gp substrate	No
CYP1A2 inhibitor	No
CYP2C19 inhibitor	No
CYP2C9 inhibitor	Yes
CYP2D6 inhibitor	No
CYP3A4 inhibitor	No
Log K_p (skin permeation)	-7.22 cm/s

Druglikeness

Lipinski	Yes; 0 violation
Ghose	Yes
Veber	No; 1 violation: TPSA>140
Egan	No; 1 violation: TPSA>131.6
Muegge	Yes
Bioavailability Score	0.56

Medicinal Chemistry

PAINS	1 alert: catechol_A
Brenk	1 alert: catechol
Leadlikeness	No; 1 violation: MW>350
Synthetic accessibility	5.52

Figure 9. Computed parameter values grouped in to different sections of the one-panel-par-molecule 2-(3,4-dihydroxyphenyl)-6-[(E)-2-(3,4-dihydroxyphenyl)ethenyl]-5'-methylspiro[2H-furo[3,2-c]pyran-3,2'-furan]-3',4-dione output (Physicochemical Properties, Lipophilicity, Pharmacokinetics, Drug-likeness and Medicinal Chemistry).

of the MDR1 gene. It leads to therapeutic failure for many drugs that are P-gp substrates [22]. Although the targeted test compound is a non-P-gp substrate, accidental increase of P-gp will not affect the therapeutic failure of the compound.

The activity of CYP enzymes is increased or decreased due to the impact of drug via altering the rate at which the drug is metabolized and removed from the body. If the drug increases the activity of a CYP protein, it causes the drug to become ineffective, due to the rapid removal of drug from the body [22]. On contrary, if the drug inhibits a CYP protein, CYP can prevent the accumulation of drug to toxic levels, even to the level of causing an overdose. Among several families of CYP proteins, CYP1, CYP2, CYP3 and CYP4 are the most essential proteins in terms of drug biotransformation; particularly CYP3A4, act as the most prevalent CYP in the body and involves in metabolizing many drugs [23]. As this compound act as a non-inhibitor for CYP3A4, it is not responsible for increasing activity of other CYP proteins allowing better absorption and clearance of the drug. Furthermore, the resulted output was compared with the

computed parameters for well-known anti cancer targeted drug lapatinib using SwissADME. Notably, computed parameters for targeted compound using SwissADME is mostly compatible with the output resulted for lapatinib drug (Figure 10).

Molecules targeting oral administration, solubility are one foremost property that influences absorption to deliver an adequate quantity of active ingredient in a small volume [24]. Moreover, it greatly facilitates various drug development activities, mostly the ease of handling and formulation. Since this targeted compound is having soluble in water, it demands for drug developmental activities.

3.5.1. BOILED-Egg Construction Model of the Molecule

The BOILED-Egg model is a perceptive graphical classification model which predicts the propensity for a given small molecule to permit passive human gastrointestinal absorption (HIA) and blood-brain barrier (BBB) permeation (Figure 11).
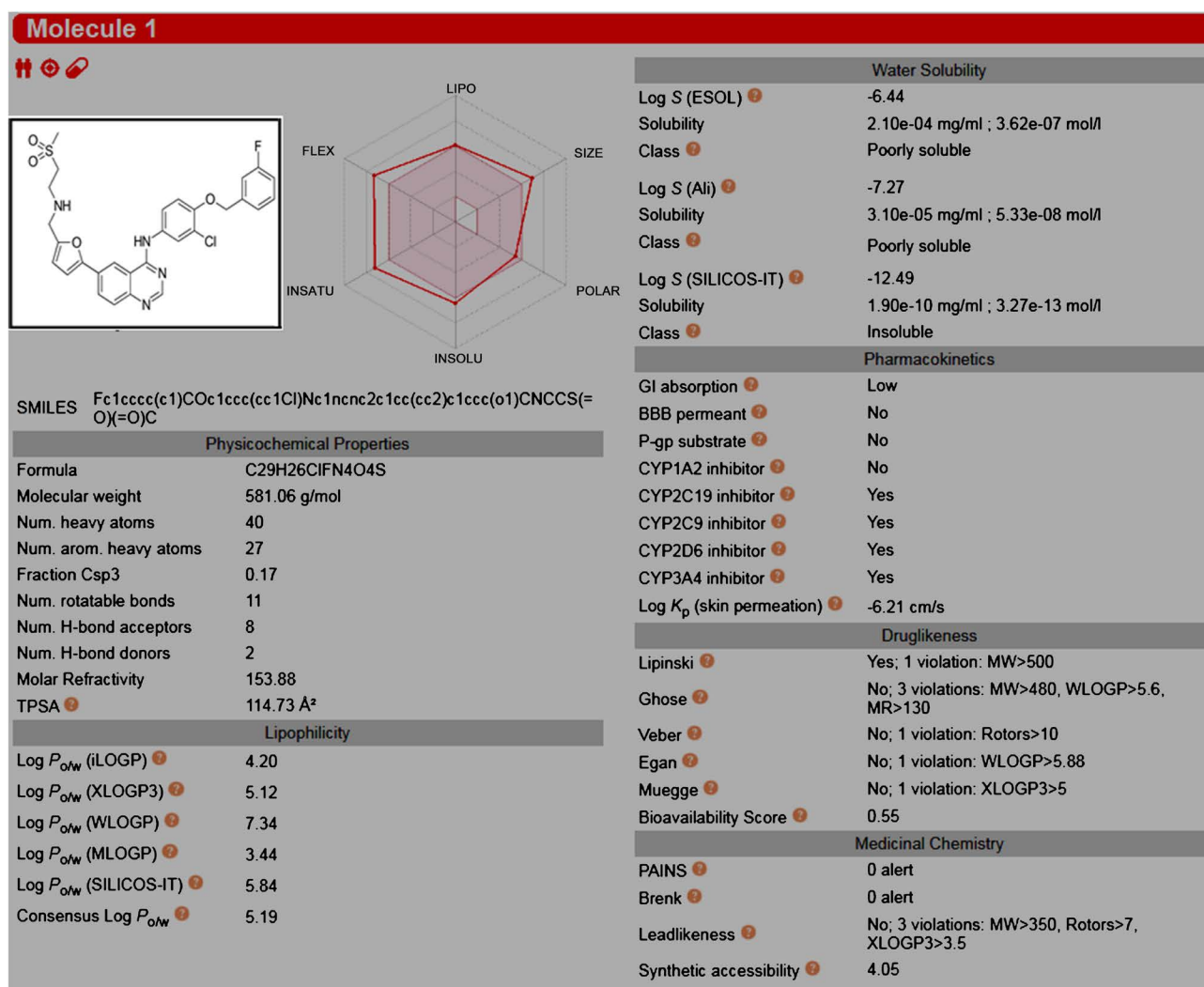

Figure 10. Computed parameter values grouped in to different sections of the one-panel-par-molecule lapatinib output (Physico-chemical Properties, Lipophilicity, Pharmacokinetics, Drug-likeness of targeted compound and Medicinal Chemistry).
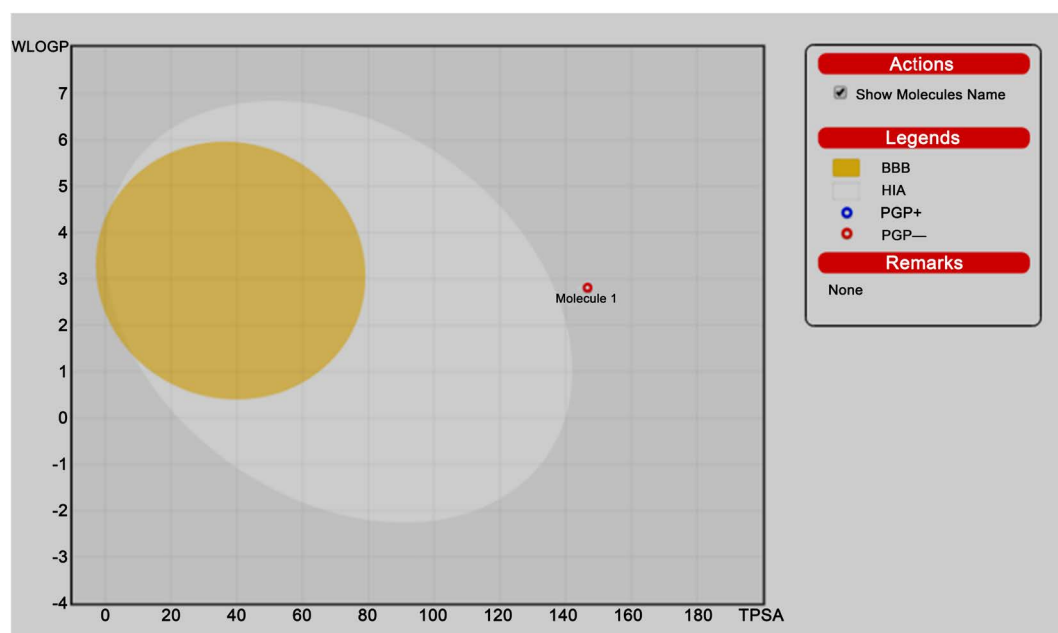
Figure 11. Overview of the BOILED-Egg construction. (a) Gastrointestinal absorption and (b) brain penetration datasets cleansed, neutralized, standardized, converted into SMILES notation were subject to lipophilicity (WLOGP) and polarity (tPSA) computation. In addition, the points are coloured in blue if predicted as actively effluxed by P-gp (PGP+) and in red if predicted as non-substrate of P-gp (PGP−).

The white region is the physicochemical space of molecules with highest probability of being absorbed by the gastrointestinal tract, and the yellow region (yolk) is the physicochemical space of molecules with highest probability to permeate to the brain. Yolk and white areas are not mutually exclusive. This model represents the tendency for 2-(3,4-dihydroxyphenyl)-6-[(E)-2-(3,4-dihydroxyphenyl)ethenyl]-5'-methylspiro[2H-furo[3,2-c]pyran-3,2'-furan]-3',4-dione in permitting passive human gastrointestinal absorption (HIA) and blood-brain barrier (BBB) permeation.

3.5.2. Prediction of Target Proteins of the Compound

It appears that Glyoxalase I, Matrix metalloproteinase 9, Matrix metalloproteinase 2 and Receptor protein-tyrosine kinase erbB-2 have a higher probability to act as target proteins for 2-(3,4-dihydroxyphenyl)-6-[(E)-2-(3,4-dihydroxyphenyl)-ethenyl]-5'-methylspiro[2H-furo[3,2-c]pyran-3,2'-furan]-3',4-dione. Moreover, Epidermal growth factor receptor erbB1 and Vascular endothelial growth factor receptor 2 were also appeared as target proteins for 2-(3,4-dihydroxyphenyl)-6-[(E)-2-(3,4-dihydroxyphenyl)ethenyl]-5'-methylspiro[2H-furo[3,2-c]pyran-3,2'-furan]-3',4-dione (Figure 12). All target proteins fit into the target classes namely enzymes, proteases, kinases, Phosphodiesterase and Lyase. Glyoxalase I is an enzyme and Matrix metalloproteinase 9, Matrix metalloproteinase 2 are proteases. Receptor protein-tyrosine kinase erbB-2; Epidermal growth factor receptor erbB1 and Vascular endothelial growth factor receptor 2 are kinases. Frequency of the target classes is represented in the pie chart given in Figure 12.
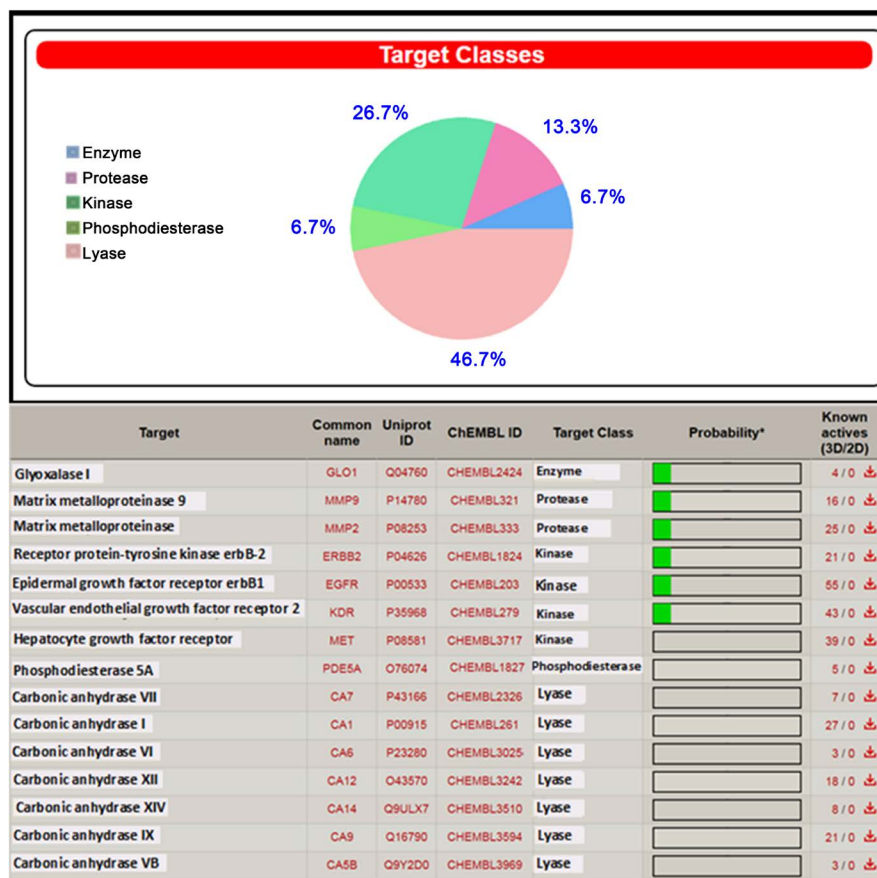
Figure 12. Target predictions for 2-(3,4-dihydroxyphenyl)-6-[(E)-2-(3,4-dihydroxyphenyl)ethenyl]-5'-methylspiro[2H-furo[3,2-c]pyran-3,2'-furan]-3',4-dione given in Swiss target prediction report. Frequency of the target classes are represented in a pie chart.

The given method is convenient and high in extraction efficiency to isolate 2-(3,4-dihydroxyphenyl)-6-[(E)-2-(3,4-dihydroxyphenyl)ethenyl]-5'-methylspiro[2H-furo[3,2-c]pyran-3,2'-furan]-3',4-dione from *Fulviformes fastuosus*. The findings of the work primarily reveal that product 2-(3,4-dihydroxyphenyl)-6-[(E)-2-(3,4-dihydroxyphenyl)ethenyl]-5'-methylspiro[2H-furo[3,2-c]pyran-3,2'-furan]-3',4-dione has novel anticancer activity against Hep-G2 cells after 24 hour treatment (IC_{50} = 20.8 μg/ml) with less cytotoxicity effect on normal CC-1 epithelial cells (SI = 3.86).

Furthermore, *in silico* study of 2-(3,4-dihydroxyphenyl)-6-[(E)-2-(3,4-dihydroxyphenyl)ethenyl]-5'-methylspiro[2H-furo[3,2-c]pyran-3,2'-furan]-3',4-dione using SwissADME has depicted that computed parameters for test compound is mostly compatible with the output resulted for well-known anticancer drug lapatinib. The above facts well imply the propensity of the product 2-(3,4-dihydroxyphenyl)-6-[(E)-2-(3,4-dihydroxyphenyl)ethenyl]-5'-methylspiro[2H-furo-[3,2-c]pyran-3,2'-furan]-3',4-dione to emerge as a safe pharmaceutical composition against hepatoma.

Moreover, SwissADME has revealed that 2-(3,4-dihydroxyphenyl)-6-[(E)-2-(3,4-dihydroxyphenyl)ethenyl]-5'-methylspiro[2H-furo[3,2-c]pyran-3,2'-furan]-

3',4-dione acts as a inhibitor for CYP2C9 protein and non-inhibitors for CYP1A2, CYP2C19, CYP2D6 and CYP3A4 proteins allowing better absorption and clearance of the targeted compound. Moreover, as test compound act as a non-substrate for P-gp/MDR1, it will not influence the therapeutic failure of the compound.

As most of the mushrooms belong to the family hymenochaetaceae, which is the family of *F. fastuosus* have been used as edible forms or are known to be non-toxic [25] [26] test compound has a greater potential to act safely in human body without producing any complications. Also, this fact was greatly supported by the high selectivity index shown by the 2-(3,4-dihydroxyphenyl)-6-[(E)-2-(3,4-dihydroxyphenyl)ethenyl]-5'-methylspiro[2H-furo[3,2-c]pyran-3,2'-furan]-3',4-dione. Accordingly, this compound can be developed as an adjuvant drug lead to use it with conventional cancer therapies. Especially, it can be directed as an active ingredient in pharmaceutical compositions including non-toxic, pharmaceutically acceptable carriers Compositions may also contain flavors, colorings and coatings. However, added agents must be non-toxic and should not interfere with the anticancer activity of the test compound [27]. Apart from it, substance can be added to fruit juice or nutrient drinks comprising nutraceuticals such as dietary supplements, vitamins and minerals.

4. Conclusion

The compound 2-(3,4-dihydroxyphenyl)-6-[(E)-2-(3,4-dihydroxyphenyl)ethenyl]-5'-methylspiro[2H-furo[3,2-c]pyran-3,2'-furan]-3',4-dione isolated from *Fulvifomes fastuosus* has shown high, novel anticancer activity on hepatoma cells with less cytotoxicity on normal CC-1 cells. *In silico* study of 2-(3,4-dihydroxyphenyl)-6-[(E)-2-(3,4-dihydroxyphenyl)ethenyl]-5'-methylspiro[2H-furo[3,2-c]pyran-3,2'-furan]-3',4-dione has shown that the test compound acts as a inhibitor for CYP2C9 protein and non-inhibitors for CYP1A2, CYP2C19, CYP2D6 and CYP3A4 proteins making better absorption and clearance of the targeted compound. Moreover, 2-(3,4-dihydroxyphenyl)-6-[(E)-2-(3,4-dihydroxyphenyl)-ethenyl]-5'-methylspiro[2H-furo[3,2-c]pyran-3,2'-furan]-3',4-dione does not possess an impact on the therapeutic failure of the compound since it acts as a non-substrate for P-gp/MDR1. Further, these computed parameters for said compound were compatible with the well-known anticancer drug lapatinib. All facts and findings are supportive to conclude that 2-(3,4-dihydroxyphenyl)-6-[(E)-2-(3,4-dihydroxyphenyl)ethenyl]-5'-methylspiro[2H-furo[3,2-c]pyran-3,2'-furan]-3',4-dione possess a high tendency to act as an adjuvant drug in the treatment of hepatoma.

Acknowledgements

Funding Statement

Conflicts of Interest

The authors declare that they have no conflicts of interests.

References

[1] Lindequist, U., Niedermeyer, T.H.J., Julich, W.D. (2005) The Pharmacological Potential of Mushrooms. *Evidence-Based Complementary and Alternative Medicine*, **2**, 285-299. https://doi.org/10.1093/ecam/neh107

[2] Figueiredo, L. and Régis, W.C.B. (2017) Medicinal Mushrooms in Adjuvant Cancer Therapies: An Approach to Anticancer Effects and Presumed Mechanisms of Action. *Nutrire*, **42**, 28-38. https://doi.org/10.1186/s41110-017-0050-1

[3] Bhanot, A., Sharma, R. and Noolvi, MN. (2011) Natural Sources as Potential Anti-Cancer Agents: A Review. *Phytomedicine*, **3**, 9-26.

[4] Reshetnikov, S.V., Wasser, S.P. and Tan, K.K. (2001) Higher Basidiomycetes as a Source of Antitumor and Immunostimulating Polysaccharides (Review). *International Journal of Medicinal Mushrooms*, **3**, 361-394. https://doi.org/10.1615/IntJMedMushr.v3.i4.80

[5] Mizuno, T. (1999) The Extraction and Development of Antitumor Active Polysaccharides from Medicinal Mushrooms in Japan-Review. *International Journal of Medicinal Mushrooms*, **1**, 9-30. https://doi.org/10.1615/IntJMedMushrooms.v1.i1.20

[6] Patel, S. and Goyal, A. (2012) Recent Developments in Mushrooms as Anti-Cancer Therapeutics: A Review. 3 *Biotech*, **2**, 1-15. https://doi.org/10.1007/s13205-011-0036-2

[7] Wasser, S.P. and Weis, A.L. (1999) Medicinal Properties of Substances Occurring in Higher Basidiomycetes Mushrooms: Current Perspectives (Review). *International Journal of Medicinal Mushrooms*, **1**, 31-62. https://doi.org/10.1615/IntJMedMushrooms.v1.i1.30

[8] Zaidman, B., Yassin, M., Mahajna, J. and Wasser, S.P. (2005) Medicinal Mushroom Modulators of Molecular Targets as Cancer Therapeutics. *Applied Microbiology and Biotechnology*, **67**, 453-468. https://doi.org/10.1007/s00253-004-1787-z

[9] Raies, A.B. and Bajic, V.B. (2016) *In Silico* Toxicology: Computational Methods for the Prediction of Chemical Toxicity. *Wiley Interdisciplinary Reviews: Computational Molecular Science*, **6**, 147-172. https://doi.org/10.1002/wcms.1240

[10] Daina, A., Michielin, O. and Zoete, V. (2017) SwissADME: A Free Web Tool to Evaluate Pharmacokinetics, Drug-Likeness and Medicinal Chemistry Friendliness of Small Molecules. *Scientific Reports*, **7**, Article No. 42717. https://doi.org/10.1038/srep42717

[11] Tian, S., Wang, J., Li, Y., Li, D., Xu, L. and Hou, T. (2015) The Application of *in Silico* Drug-Likeness Predictions in Pharmaceutical Research. *Advanced Drug Delivery Reviews*, **86**, 2-10. https://doi.org/10.1016/j.addr.2015.01.009

[12] Lipinski, C.A., Lombardo, F., Dominy, B.W. and Feeney, P.J. (2001) Experimental and Computational Approaches to Estimate Solubility and Permeability in Drug Discovery and Development Settings. *Advanced Drug Delivery Reviews*, **46**, 3-26.

[13] Hay, M., Thomas, D.W, Hay, M., Thomas, D.W, Craighead, J.L., Economides, C. and Rosenthal, J. (2014) Clinical Development Success Rates for Investigational Drugs. *Nature Biotechnology*, **32**, 40-51. https://doi.org/10.1038/nbt.2786

[14] Clark, A.M., Dole, K., Coulon-Spektor, A., McNutt, A., Grass, G., *et al.* (2015) Open Source Bayesian Models. 1. Application to ADME/Tox and Drug Discovery Datasets. *Journal of Chemical Information and Modeling*, **55**, 1231-1245. https://doi.org/10.1021/acs.jcim.5b00143

[15] Dahlin, J.L., Inglese, J. and Walters, M.A. (2015) Mitigating Risk in Academic Preclinical Drug Discovery. *Nature Reviews Drug Discovery*, **14**, 279-294. https://doi.org/10.1038/nrd4578

[16] Li, A.P. (2001) Screening for Human ADME/Tox Drug Properties in Drug Discovery. *Drug Discovery Today*, **6**, 357-366. https://doi.org/10.1016/S1359-6446(01)01712-3

[17] Badisa, R.B., Darling-Reed, S.F., Joseph, P., Cooperwood, S., Latinwo, L.M. and Goodman, C.B. (2009) Selective Cytotoxic Activities of Two Novel Synthetic Drugs on Human Breast Carcinoma MCF-7 Cells. *Anticancer Research*, **29**, 2993-2996.

[18] Kim, J., Yun, B., Shim, Y.K. and Yoo, I. (1999) Inoscavin A, A New Free Radical Scavenger from the Mushroom *lnonotus xeranticus. Tetrahedron Letters*, **40**, 6643-6666. https://doi.org/10.1016/S0040-4039(99)01406-9

[19] Fruijtier, C. (2005) Safety Assessment on Polyethylene Glycols (PEGs) and Their Derivatives as Used in Cosmetic Products. *Toxicology*, **214**, 1-38. https://doi.org/10.1016/j.tox.2005.06.001

[20] Compton, M.M. (1992) A Biochemical Hallmark of Apoptosis: Internucleosomal Degradation of the Genome. *Cancer and Metastasis Reviews*, **11**, 105-109. https://doi.org/10.1007/BF00048058

[21] Waterbeemd, H.V. and Gifford, E. (2003) ADMET *in Silico* Modelling: Towards Prediction Paradise? *Nature Reviews Drug Discovery*, **2**, 192-204. https://doi.org/10.1038/nrd1032

[22] Smith, D.A., Ackland, M.J. and Jones, B.C. (1997) Properties of Cytochrome P450 Isoenzymes and Their Substrates Part 1: Active Site Characteristics. *Drug Discovery Today*, **2**, 406-414. https://doi.org/10.1016/S1359-6446(97)01081-7

[23] Keseru, G.M. (2001) A Virtual High Throughput Screen for High Affinity Cytochrome P450cam Substrates. Implications for *in Silico* Prediction of Drug Metabolism. *Journal of Computer-Aided Molecular Design*, **15**, 649-657. https://doi.org/10.1023/A:1011911204383

[24] Hardman, J.G., Limbird, L.E., Gilman, A.G. and McGraw, H. (2001) Goodman and Gilman's "The Pharmacological Basis of Therapeutics". 10th Edition, McGraw-Hill, New York, 1392-1393.

[25] Ao, T., Ajungla, J.S.T. and Deb, C.R. (2016) Diversity of Wild Mushrooms in Nagaland, India. *Open Journal of Forestry*, **6**, 404-419. https://doi.org/10.4236/ojf.2016.65032

[26] Larsson, K., Parmasto, E., Fischer, M., Langer, E., Nakasone, K.K. and Redhead, S.A. (2006) Hymenochaetales: A Molecular Phylogeny for the Hymenochaetoid Clade. *Mycologia*, **98**, 926-936. https://doi.org/10.1080/15572536.2006.11832622

[27] Descamps, C., Cabrera, G., Depierreux, M. and Deviere, J. (2000) Acute Renal Insufficiency after Colon Cleansing. Endoscopy-Unusual Cases and Technical Notes. http://www.thieme.de/endoscopy/0200/uctn 03.html